APPLIED PHYSICS LETTERS **87**, 193508 (2005)

High-performance organic thin-film transistors with metal oxide/metal bilayer electrode

Chih-Wei Chu, Sheng-Han Li, Chieh-Wei Chen, Vishal Shrotriya, and Yang Yang[a)]
Department of Materials Science and Engineering, University of California, Los Angeles, Los Angeles, California 90095

(Received 13 June 2005; accepted 26 September 2005; published online 3 November 2005)

We demonstrate bilayer source-drain (*S-D*) electrodes for organic thin film transistors (OTFT). The bilayer consists of a transition metal oxide (MoO_3, WO_3, or V_2O_5) layer and a metal layer. The metal oxide layer, directly contacting the organic semiconducting layer, serves as the charge-injection layer. The overcoated metal layer is responsible for the conduction of charge carriers. We found that the metal oxide layer coupled between pentacene and metal layers played an important role in improving the field-effect transistor characteristics of OTFTs. Devices with the bilayer *S-D* electrodes showed enhanced hole-injection compared to those with only metal electrode. High field-effect mobility of 0.4 $cm^2/V\,s$ and on/off current ratios of 10^4 were obtained in the pentacene based TFTs using the bilayer *S-D* electrodes at a gate bias of −40 V. The improvement is attributed to the reduction in the contact barrier and the prevention of metal diffusion into the organic layer and/or unfavorable chemical reaction between the organic layer and the metal electrode. © *2005 American Institute of Physics*. [DOI: 10.1063/1.2126140]

Substantial progress has been made in developing high-performance organic semiconductors in the past decade.[1–3] Organic semiconducting materials have been used to fabricate transistors, with electronic properties similar to hydrogenated amorphous silicon (*a*-Si:H), a material often used for flat panel displays. For example, field-effect mobilities greater than 1 $cm^2/V\,s$ with large on/off current ratio have been reported for pentacene thin film transistors (TFTs).[4] Such comparable electronic characteristics, together with the advantage of low temperature and low cost fabrication on various conformable substrates, make organic thin film transistors (OTFTs) attractive candidates for use in commercial products. Although a large number of studies have focused on improving the intrinsic electrical properties of the organic semiconductors and towards the development of device fabrication techniques,[4,5] the contact between the electrodes and the active layer, which is critical to OTFT device performance, has not received much attention.

The range of electronic properties of the transition metal oxides offers a unique opportunity to control the work function, and hence, the charge-injection properties. Therefore, modification of the organic/electrode interface by inserting a transition metal oxide has received considerable attention in regards to organic electroluminescent devices.[6,7] Similarly, the source-drain (*S-D*) contacts in the organic TFTs have significant influence on device operation, through their contribution to the contact resistance arising from mismatch of the work functions, and/or interaction between the metal electrodes and the organic semiconductor.[8,9] Inserting a transition metal oxide, such as MoO_3, between the *S-D* contact and organic active layer can greatly reduce the contact resistance for the organic TFTs.

Aluminum (Al) is a well-known contact material in integrated circuits and exhibits good corrosion resistance. However, its low-work function precludes the application of Al to high performance OTFT for *P*-type semiconductors. On the other hand, high performance OTFTs can be achieved by inserting a transition metal oxide layer between Al *S-D* electrodes and organic semiconductors. In this letter, we show that the performance of OTFTs with the MoO_3/Al *S-D* electrodes greatly improved over those ones with Al, or even gold (Au), as the *S-D* electrodes. The presence of MoO_3 layer at the organic/Al interface significantly reduces the contact barrier and provides protection from diffusion and other chemical reactions between the organic layer and the metal.

The schematic structure of top-contact pentacene TFT and the energy level diagram are shown in Figs. 1(a) and 1(b). The devices were made using heavily-doped *P*-type silicon wafers with a 300-nm-thick SiO_2, which functioned as the gate electrode and the gate insulator, respectively. Prior to pentacene active layer deposition, the SiO_2 surface was cleaned by UV/O_3 cleaner and chemically-modified using silane coupling agent octadecyltrichlorosilane.[4] Following the gate insulator treatment, a 40-nm-thick layer of pentacene (Sigma-Aldrich, ~98% purity) was thermally evaporated at the rate of 0.5 Å/s from a molybdenum boat. Finally, MoO_3 (Sigma-Aldrich, 99.99% purity) and Al were thermally evaporated onto the pentacene film through a shadow mask to form the *S-D* electrodes with a channel length of 100 μm and width of 5 mm. The thicknesses of MoO_3 and Al films were 20 and 50 nm, respectively. In addition, Au and Al were investigated as alternatives to the MoO_3/Al as *S-D* contacts. All the materials were used without any further purification. All thermal evaporations were done under a pressure of less than 6×10^{-6} Torr while monitoring the film thickness with a quartz oscillator. Electrical measurements were performed in a vacuum of 10^{-5} Torr at the room temperature using an HP 4155B semiconductor parameter analyzer.

Figure 2(a) shows the source-drain current (I_{DS}) versus source-drain voltage (V_{DS}) of the OTFT with Al/MoO_3 as the *S-D* electrodes at different gate voltages (V_G). The device showed typical *P*-channel characteristics. As can be noted,

a)Electronic mail: yangy@ucla.edu

 © 2005 American Institute of Physics
Downloaded 06 Jun 2006 to 164.67.193.45. Redistribution subject to AIP license or copyright, see http://apl.aip.org/apl/copyright.jsp

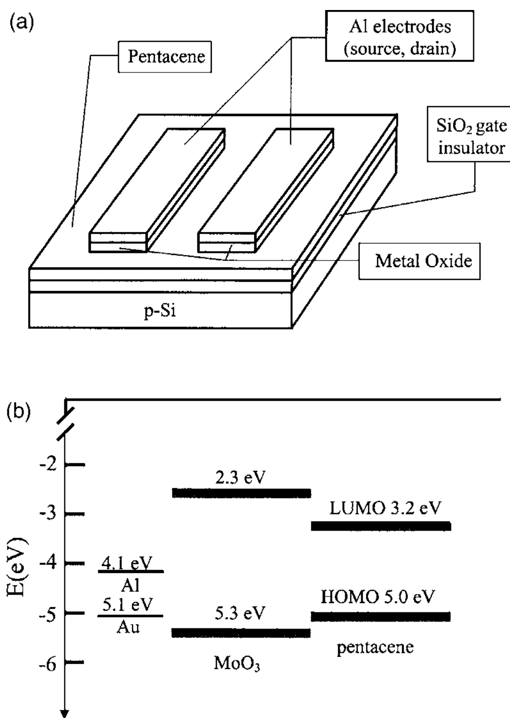

FIG. 1. (a) Structure of the organic thin film transistor; (b) energy level diagrams of pentacene, MoO_3 and the metals (Al, Au).

the output characteristics displayed very good, clear saturation currents which behaved quadratically as a function of the gate bias. The corresponding plots of $-I_{DS}$ and $(-I_{DS})^{1/2}$ versus V_G for the device are shown in Fig. 2(b). Strong field-effect modulation of the channel conductance was observed, with on/off current ratios (I_{on}/I_{off}) as high as 10^4 (measured between gate voltage, $V_G=-40$–10). The field-effect mobility (μ) was calculated at the saturation regions from the following equation:[10]

$$I_{DS} = (WC_i/2L)\mu(V_G - V_T)^2,$$

where C_i is the capacitance per unit area of the insulator, and V_T is the threshold voltage. The field-effect mobility and the threshold voltage of the OTFT were $0.40\ \text{cm}^2/\text{V s}$ and -10.43 V, respectively. On the other hand, Figs. 3(a) and 3(b) show I_{DS} versus V_{DS} curves for the OTFTs with Au and Al as the *S-D* electrodes, respectively. Both these devices showed typical *P*-channel characteristics as well. The transfer characteristics for different materials for the *S-D* electrodes are shown in Figs. 4(a) and 4(b). The device with Au *S-D* electrode had similar I_{on}/I_{0ff} compared to the device with MoO_3/Al *S-D* electrode, while I_{on}/I_{off} for the Al electrode was 10^2. In addition, the decreased slope of the transfer characteristics corresponded to a twofold decrease in the field-effect mobility to $\mu_h=0.18\ \text{cm}^2/\text{V s}$ for the Au contacts. For the case of Al, the saturation current of the channel further reduced, and field-effect mobility of $2.8 \times 10^{-3}\ \text{cm}^2/\text{V s}$ was calculated. These results demonstrate that the introduction of the metal oxide in our OTFTs played an important role in decreasing the contact resistance. Other metal oxides were combined with Al for the *S-D* electrodes and the electrical characteristics of the OTFTs with different *S-D* electrodes in this study are summarized in Table I.

In order to understand the performance improvement in the devices with MoO_3/Al as electrodes, we must consider the electronic properties of the transition metal oxide. The energy level diagrams for pentacene, MoO_3, Au, and Al are illustrated in Fig. 1(b). MoO_3 is a wide gap semiconductor with band gap of 3–3.1 eV, and an electron affinity of around 2.2 eV,[11,12] which implies the valance band position at around 5.3 eV. The highest occupied molecular orbital (HOMO) of pentacene lies at 5.0 eV (Ref. 13) and is aligned with the valence band of MoO_3, resulting in no barrier for injection of holes into the pentacene layer. It has been suggested that the excess constituent can act as doping centers

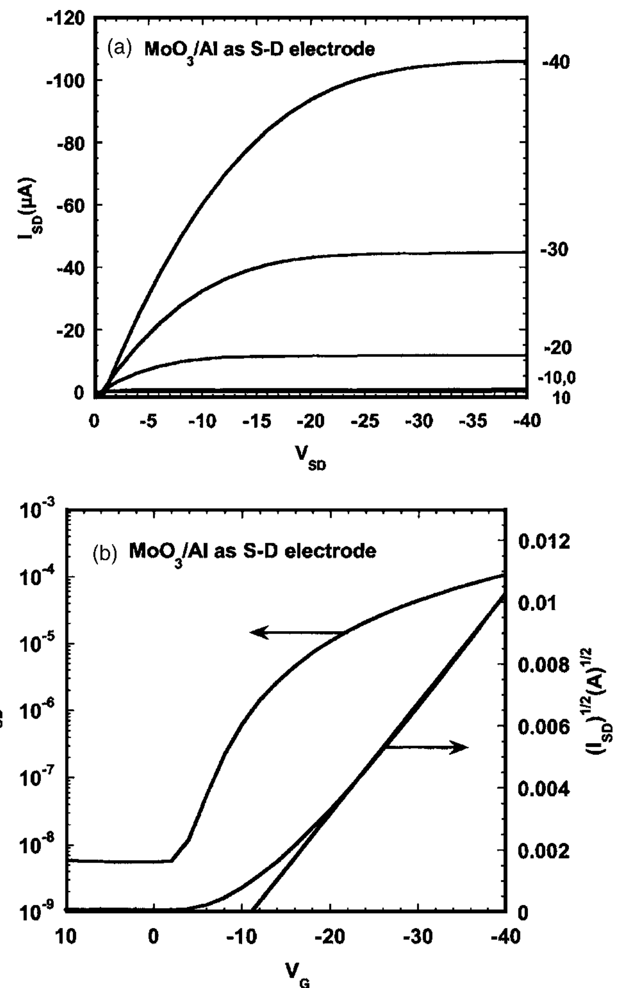

FIG. 2. (a) Source-drain current-voltage characteristics of the OTFT with MoO_3/Al electrodes. (b) The transfer characteristics of the OTFT with MoO_3/Al electrodes at a constant drain voltage of −40 V.

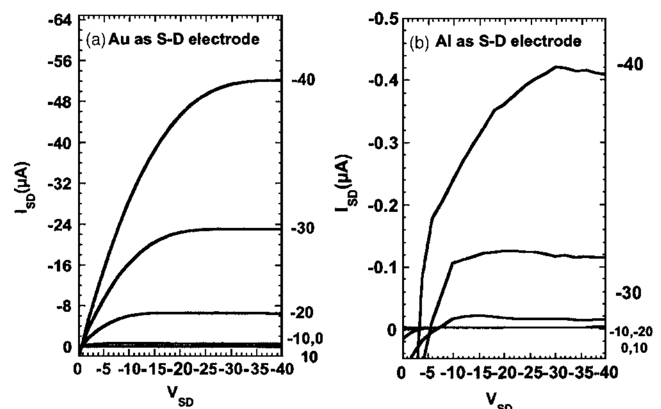

FIG. 3. Source-drain current-voltage characteristics of the OTFT where the source-drain electrodes are: (a) Au and (b) Al.

Downloaded 06 Jun 2006 to 164.67.193.45. Redistribution subject to AIP license or copyright, see http://apl.aip.org/apl/copyright.jsp

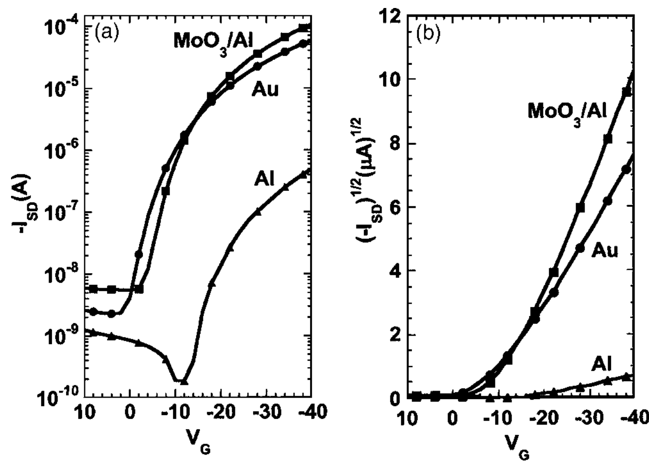

FIG. 4. Transfer characteristics for different materials as the source-drain contacts MoO3/Al (■); Au (●); Al (▲): (a) $-I_{SD}-V_G$ and (b) $(-I_{SD})^{1/2}-V_G$ plots at $V_D=-40$ V.

and that this dopant controls the electrical properties of the film.[14,15] Since MoO_3 layer was deposited by evaporation, MoO_3 yields a film containing species from MoO to MoO_3 as well as free Mo. Additionally, impurities might be introduced into the film, arising from boats used during thermal evaporation, as well as from the impurities present in MoO_3 powder. The width of the depletion region between metal and MoO_3 junction decreases as the doping concentration in the MoO_3 film increases; as a result, the probability of tunneling through the barrier increases. Therefore, an Ohmic contact is likely to be achieved at the metal and MoO_3 interface. To further demonstrate this, devices were fabricated using MoO_3 covered with different metals (Au, Ag, and Al) as the electrodes. Figure 5 shows the transfer characteristics of OTFTs using MoO_3 covered with different metals as the electrodes. They show similar electrical characteristics and improved performance compared to metal-only electrodes.

Because of the small mismatch between the work function of Au and the HOMO level of pentacene, Au is one of the most promising metal electrodes for pentacene TFTs. However, metals deposited onto the pentacene surface either penetrate the surface, thereby doping the upper layer of pentacene, or diffuse into pentacene to form a metallic overlayer, which is a mixture of metal and pentacene instead of pure metal. The interface dipole immediately forms increasing the barrier height between metal and pentacene.[16] The modified MoO_3 layer interface provides protection against metal diffusion into the organic layer and an unfavorable chemical reaction between organic and metal electrodes. The modification decreases the intensity of interface dipole and enhances charge injection.

TABLE I. Electrical parameters of the OTFTs in this study.

Drain-source electrodes	Mobility ($cm^2/V\,s$)	Threshold voltage (V)	On-off ratio
Al	2.8×10^{-3}	−16.2	2.3×10^{2}
Au	0.182	−8.75	2.8×10^{4}
MoO_3/Al	0.4	−12.1	3.8×10^{4}
WO_3/Al	0.253	−12.88	4.1×10^{4}
V_2O_5/Al	0.226	−10.43	1.8×10^{4}

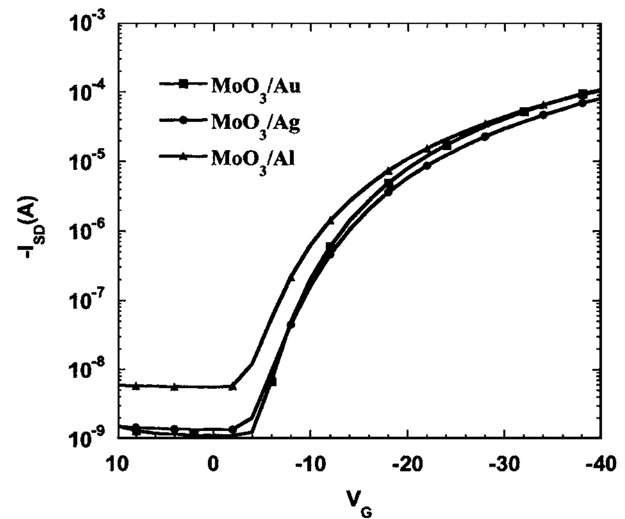

FIG. 5. Transfer characteristics ($-I_{SD}$ vs V_G) of OTFTs using MoO_3 covered with different metals as the electrodes. MoO_3/Au (●); MoO_3/Ag (■); MoO_3/Al (▲).

In conclusion, the OTFTs with MoO_3 as a hole injection layer between the metal electrodes and the organic semiconductor layer were fabricated through thermal evaporation. Compared with OTFTs without the metal oxide, the current and the field-effect mobility were significantly improved. Therefore, using a transition metal oxide as the hole injection layer is an effective way to improve the characteristics of OTFTs, making the device suitable for commercial applications.

Financial support from the Air Force of Scientific Research (Program manager Dr. Charles Lee, Grant No. F49620-03-1-0101) is deeply appreciated. C.W.C is also grateful for the financial support from MediaTek Fellowship.

[1] C. W. Tang and S. Van Slyke, Appl. Phys. Lett. **51**, 913 (1987).
[2] P. Peumans, A. Yakimov, and S. R. Forrest, J. Appl. Phys. **93**, 3693 (2003).
[3] H. E. Katz and Z. Bao, J. Phys. Chem. B **104**, 671 (2000).
[4] Y. Lin, D. J. Gundlach, S. F. Nelson, and T. N. Jackson, IEEE Trans. Electron Devices **18**, 606 (1997).
[5] M. Shtein, J. Mapei, J. B. Benziger, and S. R. Forrest, Appl. Phys. Lett. **81**, 268 (2002).
[6] J. Kido, T. Matsumoto, T. Nakada, J. Endo, K. Mori, N. Kawamura, and A. Yoko, SID Int. Symp. Digest Tech. Papers **34**, 964 (2003).
[7] G. L. Frey, K. J. Reynolds, and R. H. Friend, Adv. Mater. (Weinheim, Ger.) **14**, 265 (2002).
[8] R. Hajlaoui, G. Horowitz, F. Garnier, A. Arce-Brouchet, L. Laigre, A. El Kassmi, F. Demanze, and F. Kouki, Adv. Mater. (Weinheim, Ger.) **9**, 389 (1997).
[9] C. Waldauf, P. Schilinsky, M. Perisutti, J. Hauch, and C. J. Brabec, Adv. Mater. (Weinheim, Ger.) **15**, 2084 (2003).
[10] S. M. Sze, *Physics of Semiconductor Devices* (Wiley, New York, 1981).
[11] T. Yasuda, T. Goto, K. Fujita, and T. Tsutsui, Appl. Phys. Lett. **85**, 2098 (2004).
[12] P. A. Cox, *Transition Metal Oxides, An Introduction to Their Electronic Structure and Properties* (Clarendon, Oxford, 1992).
[13] A. Galtayries, S. Wisniewski, and J. Grimblot, J. Electron Spectrosc. Relat. Phenom. **87**, 31 (1997).
[14] J. G. Simmons, Phys. Rev. **166**, 912 (1968).
[15] G. S. Nadkarni and J. G. Simmons, J. Appl. Phys. **41**, 545 (1970).
[16] N. J. Watkins, L. Yan, and Y. L Gao, Appl. Phys. Lett. **80**, 4384 (2002).

Downloaded 06 Jun 2006 to 164.67.193.45. Redistribution subject to AIP license or copyright, see http://apl.aip.org/apl/copyright.jsp